

# Validation Results of Pressure Independent First-Order Thermal Models of High-Altitude Balloon Gondolas

Jeremy Meduvsky<sup>1</sup>, Michael Howeth<sup>2</sup>, Chelsea Katan<sup>3</sup>, Douglas R. Isenberg<sup>4</sup>  
*Embry-Riddle Aeronautical University, Prescott, AZ, 86301*

**This paper discusses the validity of pressure independent first-order thermal models for high-altitude balloon gondolas subjected to short duration flights. Thermal system identification results performed on a test gondola in a vacuum chamber at varying pressures are presented. These results indicate that the lumped parameter of thermal resistance changes significantly with pressure. Though this dependence on pressure may make a difference on long-duration flights, the validation results that are presented in this paper indicate that pressure independent models are capable of responding to within a few degrees of the actual temperature on short duration flights.**

## I. Introduction

The thermal properties of high-altitude balloon gondolas have been an area of study since the 1960's [1-4]. Much of the earlier work focused on long duration flights in the high-atmosphere in which gondolas cycle through significant periods of radiative heating during the day and radiative cooling at night. More recently, short duration flights have become very common for educational purposes. Gondolas on these flights are not subjected to long periods of intense radiative heating or cooling. Instead, these short, several-hour-long flights are characterized by a quick ascent followed by a quick descent with relatively little time spent floating in the upper atmosphere. Thus, the heat transfer dynamics on these flights are largely governed by the combined effects of forced-air convective cooling during the ascent and descent, solar radiative heating, and conduction within the gondola structure. Since it is typically the case that a small volume of the gondola is the only section where the temperature may be of any major significance, a particular volume is selected and treated as an isothermal node characterized by a constant thermal capacitance with the combined effects of the various heat transfers into and out of the node lumped into a constant thermal resistance [5]. This effectively reduces the complex heat transfer process into a single dimensional process that is described by a linear first-order ordinary differential equation for which the thermal resistance and thermal capacitance of the isothermal node can be easily found via simple experimental methods [6]. This paper provides evidence to support the validity of this system modeling and identification procedure carried out at ground-level atmospheric pressure.

This paper is organized in the following manner. First, the modeling and identification process is reviewed. The heat transfer equation is developed and the experimental procedure and subsequent numerical technique for identifying the process constants are discussed. Next, laboratory results from carrying out the procedure on a hollow sphere inside of a vacuum chamber are presented. Interestingly, these results indicate that the lumped thermal capacitance is relatively constant with pressure while the thermal resistance does change significantly with pressure. Since the effectiveness of any modeling and parameter identification procedure is evaluated by how well the resulting model replicates the phenomenon that is being modeled, the models for three different gondolas are validated with actual flight data. The paper then concludes with a few observations and recommendations for future work.

## II. Thermal Modeling and Identification

The modeling and identification procedure for high altitude gondolas that is summarized below was first described in [6]. The only instrumentation required to carry out the experimental portion of the procedure are two temperature sensors making it an attractive option for academic laboratories. The system identification portion of

---

<sup>1</sup> Student, Dept. of Aerospace and Mechanical Engineering, meduvskj@my.erau.edu

<sup>2</sup> Student, Dept. of Aerospace and Mechanical Engineering, howethm@my.erau.edu

<sup>3</sup> Student, Dept. of Aerospace and Mechanical Engineering, katan@my.erau.edu

<sup>4</sup> Assistant Professor, Dept. of Aerospace and Mechanical Engineering, [isenberd@erau.edu](mailto:isenberd@erau.edu), AIAA Member

the process can be performed on paper utilizing the time-constant identification method for first-order systems, however, better results can be obtained by using numerical optimization algorithms on a personal computer.

In order to develop the analytical heat transfer model, first consider the diagram in Figure 1. The simplified model consists of a single isothermal node, which will be denoted as the payload, with a temperature,  $T$ , and a thermal capacitance,  $C$ . In practice, this isothermal node has typically been selected as the data-logging circuit. A heat source inside the gondola applies heat,  $Q_H$ , directly to the payload. This heat source is due to power dissipated by any resistive circuits inside the gondola which includes the power dissipated by the payload itself as well as any additional heating elements that may be intentionally placed inside the gondola. The gondola is a structure with insulating properties that shields the payload from the outside atmosphere of temperature,  $T_{out}$ , and solar radiation,  $Q_{sun}$ .

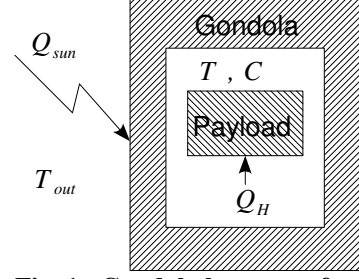


**Fig. 1: Gondola heat transfer.**

Heat is lost from the payload to the atmosphere inside the gondola and to the inside surface of the gondola structure itself via convection and radiation, respectively. Furthermore, heat is transferred from the inner gondola surface to the outer gondola surface via conduction. In addition, heat is lost from the outer surface of the gondola to the atmosphere via convection, and to space via radiation. Heat is stored in the payload, the atmosphere inside the gondola, and the gondola structure. The ability of the payload and gondola to store heat is invariant to pressure, but the ability of the atmosphere inside the gondola to store heat will obviously be dependent upon the atmospheric pressure. The effects of pressure are discussed in the next section.

Each of the heat transfer processes taking place in the system is lumped into a single thermal resistance,  $R$ , with units  $(K/W)$ , and the combined ability to store heat in the payload is lumped into a single thermal capacitance,  $C$ , with units  $(J/K)$ . Knowing that the heat stored must be equal to the heat entering minus the heat leaving the system, the heat transfer dynamical equation is formulated as

$$C \dot{T}(t) = -\frac{1}{R}(T(t) - T_{out}(t)) + Q_H(t) + Q_{sun}(t). \quad (1)$$

Equation (1) is a reduced-order model that is intended to capture the significant features of the dynamic response. By adjusting the values of  $C$ ,  $R$ , and  $Q_{sun}$ , we seek to find the best fit in the least-squares sense of the step-response of (1) with an experimentally measured step-response of actual system. In order to do this, the identification process is decomposed into two separate experiments. The first experiment is carried out with no direct sunlight so that,  $Q_{sun} = 0$  ( $W$ ). A known internal heat source is applied to the inside of the gondola so that  $Q_H$  is constant. This is easily accomplished with a fixed resistance and a fixed voltage source. For academic laboratory experiments,  $Q_H$  is typically set to approximately 5 ( $W$ ). The heat source is instantaneously applied and measurements of the payload temperature,  $T_{meas}(t)$ , and outside temperature,  $T_{out}(t)$ , are periodically recorded. Since  $T_{out}(t)$  should ideally be constant in a laboratory setting but may fluctuate slightly due to various uncontrolled factors, it is advisable to find and utilize its time-averaged value,  $\hat{T}_{out} = \text{mean}(T_{out}(t))$ , as a constant. Since  $T_{out}$ ,  $Q_H$ , and  $Q_{sun}$  are assumed constant, then the solution to (1) has the form,

$$T(t) = (T(0) - a_2) e^{\frac{-t}{a_1}} + a_2, \quad (2)$$

where  $a_1 = RC$  and  $a_2 = T(\infty)$  are unknown but will be determined via numerical optimization. Assume that  $n+1$  samples are taken including the initial value,  $T_{meas}(0)$ . Then, define the error between the approximated model in (2) and actual system response as the  $n \times 1$  vector:

$$\underline{e} = \begin{bmatrix} T_{meas}(t_1) - \left( (T_{meas}(0) - a_2) e^{\frac{-t_1}{a_1}} + a_2 \right) \\ T_{meas}(t_2) - \left( (T_{meas}(0) - a_2) e^{\frac{-t_2}{a_1}} + a_2 \right) \\ \vdots \\ T_{meas}(t_n) - \left( (T_{meas}(0) - a_2) e^{\frac{-t_n}{a_1}} + a_2 \right) \end{bmatrix}. \quad (3)$$

The objective is to find the values of  $a_1$  and  $a_2$  that minimize  $\|\underline{e}\|^2$ . This can be accomplished via a variety of minimization algorithms. The authors have found that the MATLAB function, `lsqnonlin`, provides satisfactory results. It is interesting to notice that it is not required to carry out the measurement portion of the experiment until

steady-state is reached. Since  $a_2=T(\infty)$ , it is only necessary to collect enough data to sufficiently characterize the shape of the best-fit exponential.

With both  $a_1=RC$  and  $a_2=T(\infty)$  obtained, it is possible to solve for the thermal resistance and thermal capacitance. At steady-state, with  $Q_{sun}=0$  (K), equation (1) becomes

$$0=-\frac{1}{R}(T(\infty)-\hat{T}_{out})+Q_H. \quad (4)$$

So, the thermal resistance is

$$R=\frac{T(\infty)-\hat{T}_{out}}{Q_H}. \quad (5)$$

Thus, the thermal capacitance is found as

$$C=\frac{a_1}{R}. \quad (6)$$

Having found values for the thermal capacitance and the thermal resistance, it is then possible to solve for  $Q_{sun}$ . For this procedure, it is helpful to zero  $Q_H$  by removing electrical power to the electronics and heating elements. Then, by placing the gondola in direct sunlight and allowing a new steady-state temperature to be reached,  $Q_{sun}$  is obtained as

$$Q_{sun}=\frac{T_{meas}(\infty)-\hat{T}_{out}}{R}. \quad (7)$$

### III. Laboratory Results

The modeling and identification procedure described in the previous section is carried out with a ground level atmospheric pressure. As previously described, several of the heat-transfer processes involved in the thermal dynamics are convective and radiative in nature. An ascending gondola experiences a drop in atmospheric pressure whereby convection becomes less significant while radiation becomes the primary method of heat transfer through non-solid space. Thus, it is evident that atmospheric pressure will have an effect on the dynamical model. In order to investigate the effects that atmospheric pressure has on the thermal capacitance and thermal resistance, the first part of the procedure described above was carried out inside a vacuum chamber nine times for nine different, but constant, pressures. The gondola that underwent the tests is a hollow fiberglass and epoxy sphere comprised of two hemispheres with an outside surface coating comprised of aluminum tape. The gondola was suspended inside the chamber to avoid conduction between the gondola's outside surface and the chamber's wall. Figure 2 depicts the nine step-responses for each of the different pressures while Table 1 tabulates the applied heat source, the identified thermal capacitance, and the identified thermal resistance for each pressure.

A useful index for quantifying the effects of pressure on the thermal resistance and thermal capacitance is the standard deviation of the data with respect to the pressure divided by the mean of the data with respect to the pressure. Carrying out these calculations, one finds:

$$\frac{std(R_p)}{mean(R_p)}=0.4406 \quad \text{and} \quad \frac{std(C_p)}{mean(C_p)}=0.0890.$$

This index is considerably larger for the thermal resistance than it is for the thermal capacitance, indicating that the pressure has significantly more effect on the lumped parameter value of thermal resistance than it does for the lumped parameter value of the thermal capacitance. The somewhat constant thermal capacitance is a good indication that the volume of gaseous atmosphere inside the gondola is not capable of holding a relatively large amount of heat. Likewise, the changing thermal resistance tends to indicate that the presence of a gaseous atmosphere inside and outside of the gondola substantially contributes to the heat-transfer processes of the system. Figure 3 depicts the identified thermal resistance and thermal capacitance plotted against pressure. The thermal resistance data has a close fit to a natural logarithmic curve, which is also plotted.

Using the best-fit logarithmic curve for thermal resistance as a function of pressure, the thermal resistance behavior during a high-altitude flight is explored in Figure 4. The top two plots depict recorded altitude versus time and pressure versus time, which are quite typical profiles for short duration flights. Using this information, the thermal resistance versus time is plotted in the third graph, and the thermal resistance versus altitude is plotted in the fourth graph.

Two very interesting and potentially useful trends regarding pressure dependency emerge from the plots in Figure 4. On the ascent phase of the flight, the thermal resistance is nearly affine with time. This trend is likely due

to the nearly constant ascent velocity along with the trend in the fourth graph which shows that the thermal resistance is nearly affine with altitude as well. This information could prove valuable in developing either a time-dependent first-order thermal model or a pressure dependent first-order thermal model.

The data from this controlled laboratory experiment indicates that lumped parameter first-order thermal models for high altitude gondolas are pressure dependent. However, the experiment did not incorporate forced-air convection on the outside of the gondola as would be experienced on the ascent and descent of a flight. The effect of forced-air convection would be to decrease the thermal resistance from its experimentally measured free-air convection value in the denser portion of the atmosphere.

#### IV. Validation

Although the experimental results described in the previous section indicate that a gondola thermal model is pressure dependent, the sufficiency of the pressure independent models can be assessed by applying real data to the models and comparing the modeled outputs with the actual outputs. This process is accomplished by utilizing the  $T_{out}$  that was measured during a flight and the identified  $Q_{sun}$  as inputs to the system described in (1) and then integrating the differential equation numerically ( $Q_H$  is typically very small but should also be included as an input if its value is within a magnitude of  $Q_{sun}$ ). Data is logged on the author's flights at a rate of 10 (Hz) which is much faster than the single pole of the identified thermal systems. Thus, it has been found from experience that a simple Euler integration is entirely sufficient for validation and very little improvement is gained by using higher-order integration methods.

The validation process is carried out for the three different gondolas depicted in Figure 5 by using the identified thermal parameters presented in Table 2. These gondolas flew one flight each on three different flights with the flights reaching approximately 30 (km), 15 (km), and 20 (km), respectively. Plots of the modeled payload temperature, actual payload temperature, and outside temperature for the three gondolas are depicted in Figure 6.

The top plot in Figure 6 depicts the temperature profile for the payload that was discussed in [5], which is referred to as "gondola 1" in this paper. This payload incorporated a bang-off feedback controller that would apply a heat of 8.1 (W) whenever the temperature dropped below 294 (K) and 0 (W) when the temperature was above 294 (K). The payload was constructed of carbon-fiber honeycomb panels, and interestingly, though it is the smallest of the three in size, it has the largest identified value for  $Q_{sun}$ .

The second plot in Figure 6 depicts the temperature profile for gondola 2. Gondola 2 is the largest in size and was constructed entirely of foam panels. It has the largest thermal capacitance and smallest thermal resistance of the three gondolas.

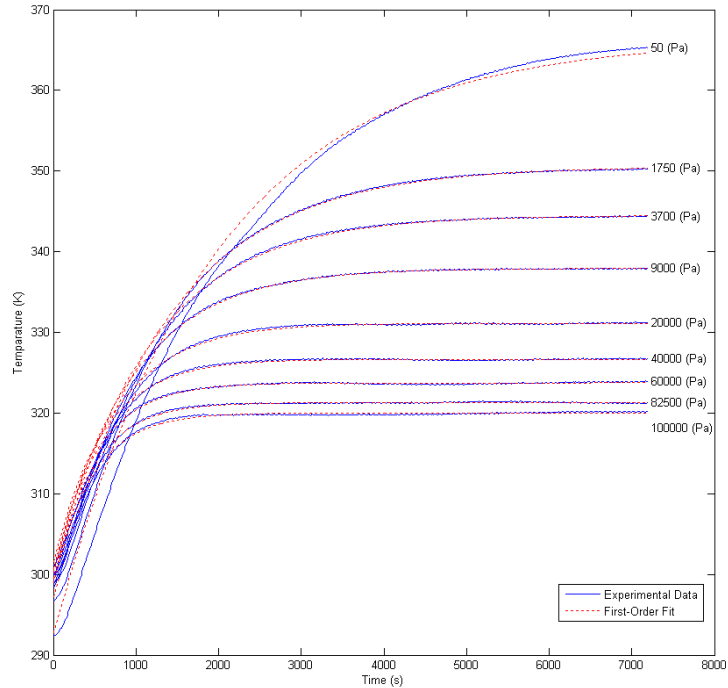


**Fig. 2: Measured and best-fit first-order step responses due to internal heat source for different pressures.**

**Table 1: Internal heat source experiment data.**

Pressure (Pa)	Heat Source (W)	Thermal Resistance (K/W)	Thermal Capacitance (J/K)
50	4.556	14.988	140.796
1750	4.674	11.164	127.799
3700	4.662	9.833	125.439
9000	4.668	8.303	119.248
20000	4.645	6.977	114.467
40000	4.678	5.887	112.379
60000	4.712	5.284	106.069
82500	4.693	4.718	111.531
100000	4.728	4.474	114.718

The third plot in Figure 6 depicts the temperature profile for gondola 3. Gondola 3 was constructed of foam board with an outside layer of fiberglass and epoxy. In addition, a layer of aluminum tape was placed on top of the fiberglass layer. This gondola had the highest thermal resistance, the lowest thermal capacitance, and the lowest value  $Q_{sun}$  of the three gondolas. The data-logging stopped abruptly about eight minutes after the balloon burst, so the entire flight temperature profile for this gondola is not available.

The plots in Figure 6 show that the modeled temperature follows the trend in the actual temperature. There is no clear indication from these results that the modeled temperature consistently leads ahead or lags behind the actual temperature. In [6], it was reported that forced-air convective cooling during descent was suspected of being responsible for the large error in the top plot that occurs around 9000 (s). Concurring evidence is seen in the bottom two plots during the ascent phase where the modeled temperature is not as cold as the actual temperature. It can also be seen in the descent phase in the middle plot that the actual temperature is a few degrees colder than the modeled temperature, which also supports the notion that the discrepancy is caused by the unmodeled effects of forced-air convection.

The percent error between the modeled temperature and the actual temperature provides an index for quantifying the effectiveness of the thermal models. The percent error for each of the plots depicted in Figure 6 is plotted in Figure 7 against the atmospheric pressure which was also measured during each flight. It can be seen that the percent error in the modeled temperature is never more than three percent. Furthermore, no clear trend arises with respect to error versus altitude. Of course, since the dynamic system is moving spatially, any error that is due to pressure dependence will not be seen at those pressures that are contributing to the error, but at pressures that are further along

**Table 2: Identified gondola thermal parameters.**

Gondola	$Q_{sun}$ (W)	$R$ (K/W)	$C$ (J/K)
1	3.189	4.803	610.17
2	2.161	2.560	980.38
3	0.733	5.724	399.42

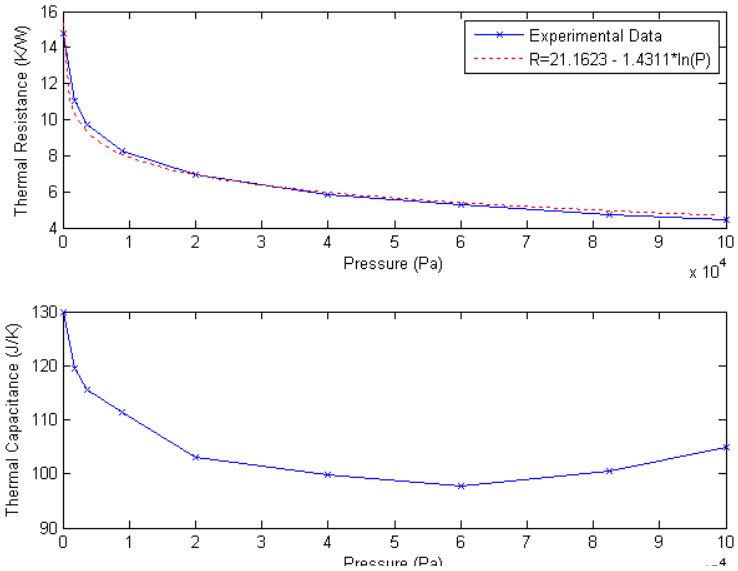


**Fig. 3: Thermal resistance and thermal capacitance vs. pressure.**

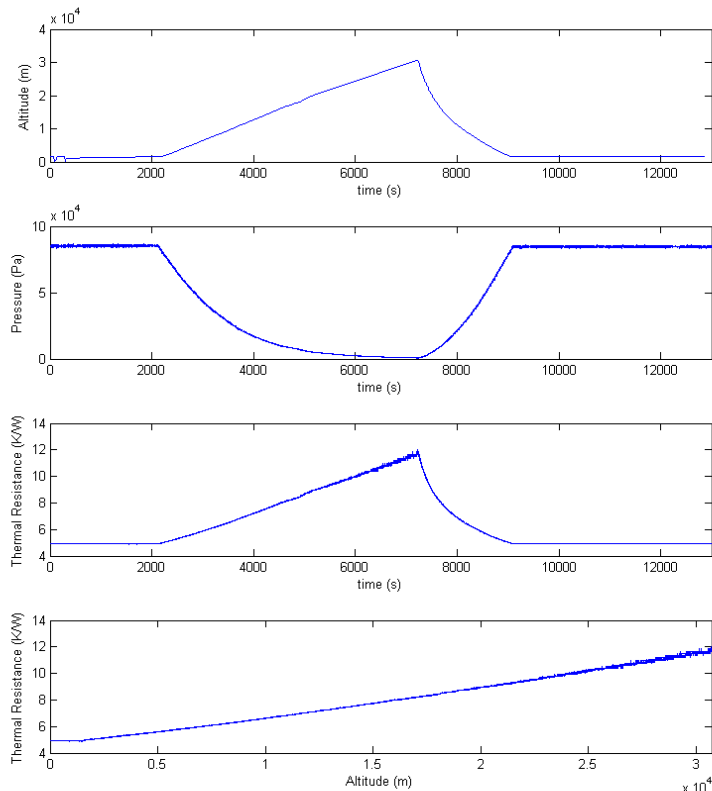


**Fig. 4: Thermal resistance and altitude relation using best-fit logarithmic trend.**



**Fig. 5: Tested gondolas.**

in the ascent and descent. Still, the relatively small percent error indicates that the first-order pressure independent thermal model provides sufficient accuracy for a cursory analysis of payload temperature in gondolas on short-duration flights.

### V. Conclusion

Ideally, a system model should exactly replicate measured variables when subjected to the same inputs as the actual system. This rarely occurs in practice. Most often, the dynamics that contribute to a system's response are approximate, unmodeled, or in the worst case, unknown. So, one is left with the task of making the subjective decision of whether or not a model is sufficient for its intended purpose. In this paper, a pressure independent first-order thermal model is examined. It is known from the basic physics of the problem being examined that a first-order model in the form of an ordinary differential equation is only a rough approximation. Furthermore, even laboratory evidence shows that thermal resistance and thermal capacitance (to a lesser degree) are functions of atmospheric pressure. Still, for the three cases examined in this paper, an identified first-order thermal model accurately predicts the temperature trends to within a few degrees Kelvin. If the intended purpose of the model is simply to determine whether or not the payload temperature on a short duration flight will stay above (or below) an acceptable value, then this type of model seems entirely adequate. Such a model should also prove to be adequate in evaluating the need (or lack thereof) for additional thermal control consideration.

The thermal identification process described in this paper seems promising, but there are still several improvements that can be made to the procedure. One such improvement would be to take into account the time and date of the solar input testing. Even on a clear day, the solar input is not constant with respect to time, though there is a span of a few hours when the solar input is at a maximum and nearly constant. Solar input tests, which typically take several hours to conduct, should be carried-out during that time of day. The value for  $Q_{sun}$  that is identified should then be appropriately scaled by the ratio of the predicted solar input at the date and time of the launch and the solar input that was observed during testing. Values for solar

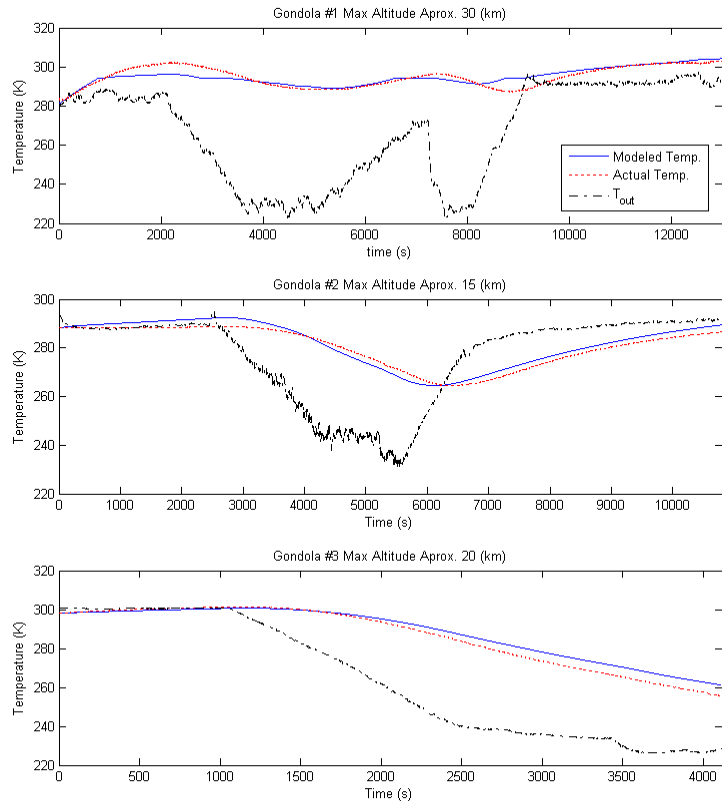


**Fig. 6: First-order heat transfer model validation results.**

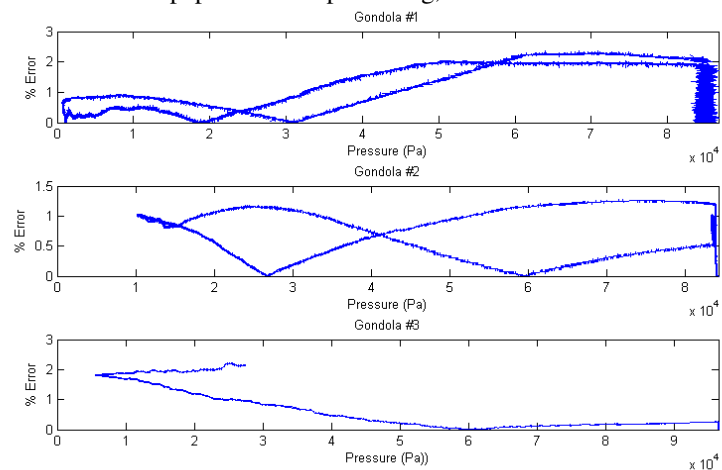


**Fig. 7: Percent error in modeled temperature error vs. pressure.**

flux at different dates and times are available from the National Renewable Energy Laboratory\*. Another possible improvement would be to incorporate the effects of pressure on the thermal resistance into the model. If the thermal resistance versus pressure curve in Figure 3 holds moderately true in all cases, then a two-point calibration procedure could be utilized to find the coefficients of  $R = \alpha + \beta \cdot \ln(P)$ . This would require that one of the step-response experiments be carried-out at a preferably lower pressure than the ground-level atmospheric pressure. If multiple step-response experiments are carried-out at different pressures, then a least-squares curve fit could be utilized. Similarly, an investigation into the effects of forced-air convection and how it varies with pressure and ascent/descent velocity would also prove useful. Of course, increasing the order of the thermal model is another option that may be worth exploring. However, the drawback to utilizing a higher-order model is the need for inputs that sufficiently excite the modes of the system, which possibly makes the identification experiments more complicated and less attractive for an instructional academic laboratory.

### References

- <sup>1</sup>Liechfield, E.W., Carlson, N.E., "Temperature Control of Balloon Packages", NCAR Technical Notes, NCAR-TN-32, 1967
- <sup>2</sup>Kreith, F., Warren, J. Thermal Analysis of Balloon-Borne Instrument Packages", NCAR Technical Notes, NCAR-TN-45, 1970
- <sup>3</sup>Carlson, L.A., "Thermal Analysis Program", *Atmospheric Technology*, No. 5, 1974, pp. 40-43
- <sup>4</sup>Carlson, L.A., Brandeberry, P.M., "Thermal Analysis of Long Duration Flight Packages", *Proceedings: 8<sup>th</sup> AFCRL Scientific Ballooning Symposium*, 1974, pp. 163-173
- <sup>5</sup>Lindsay, J.F., Katz, S., *Dynamics of Physical Circuits and Systems*, Matrix Publishers, Inc., Champaign, IL, 1978
- <sup>6</sup>Isenberg, D.R., Rookaird, B.M., Weisshaupt, J., Smith, J., Winterling, B., "Identifying the Thermal Parameters and Controlling the Temperature of a High-Altitude Balloon Payload", *Proceedings: 3<sup>rd</sup> Annual Academic High-Altitude Conference*, 2012, pp. 1-14

---

\* <http://www.nrel.gov/midc/solpos/solpos.html>